Chromatin remodelers clear nucleosomes from intrinsically unfavorable sites to establish nucleosome-depleted regions at promoters

Denis Tolkunov[a,*], Karl A. Zawadzki[b,*,†], Cara Singer[b], Nils Elfving[b], Alexandre V. Morozov[a], and James R. Broach[b]

[a]Department of Physics and Astronomy and BioMaPS Institute for Quantitative Biology, Rutgers University, Piscataway, NJ 08854; [b]Department of Molecular Biology, Princeton University, Princeton, NJ 08544

ABSTRACT **Most promoters in yeast contain a nucleosome-depleted region (NDR), but the mechanisms by which NDRs are established and maintained in vivo are currently unclear. We have examined how genome-wide nucleosome placement is altered in the absence of two distinct types of nucleosome remodeling activity. In mutants of both *SNF2*, which encodes the ATPase component of the Swi/Snf remodeling complex, and *ASF1*, which encodes a histone chaperone, distinct sets of gene promoters carry excess nucleosomes in their NDRs relative to wild-type. In *snf2* mutants, excess promoter nucleosomes correlate with reduced gene expression. In both mutants, the excess nucleosomes occupy DNA sequences that are energetically less favorable for nucleosome formation, indicating that intrinsic histone–DNA interactions are not sufficient for nucleosome positioning in vivo, and that Snf2 and Asf1 promote thermodynamic equilibration of nucleosomal arrays. Cells lacking *SNF2* or *ASF1* still accomplish the changes in promoter nucleosome structure associated with large-scale transcriptional reprogramming. However, chromatin reorganization in the mutants is reduced in extent compared to wild-type cells, even though transcriptional changes proceed normally. In summary, active remodeling is required for distributing nucleosomes to energetically favorable positions in vivo and for reorganizing chromatin in response to changes in transcriptional activity.**

Monitoring Editor
Fred Chang
Columbia University

Received: Oct 15, 2010
Revised: Apr 7, 2011
Accepted: Apr 11, 2011

INTRODUCTION

DNA sequences upstream of the transcription start site of most genes in yeast and other eukaryotes are depleted of nucleosomes (Cairns, 2009; Clapier and Cairns, 2009; Rando and Chang, 2009; Tolkunov and Morozov, 2010). These nucleosome-depleted regions (NDRs) are flanked by two well-positioned nucleosomes: the +1 nucleosome, which overlaps the transcription start site, and the −1 nucleosome, which occurs at a characteristic distance further upstream (Mavrich *et al.*, 2008). NDRs often contain transcription factor binding sites and the accessibility of these sites allows appropriate response of genes to changes in the transcription factor activity or local concentration (Zawadzki *et al.*, 2009). Similarly, nucleosome occlusion of spurious transcription factor binding sites at nonpromoter regions of the genome precludes inappropriate transcriptional activation from nonfunctional domains (Liu *et al.*, 2006; Whitehouse *et al.*, 2007; Zawadzki *et al.*, 2009). Repressed genes generally contain NDRs, allowing initial interaction with transcription factors during activation (Korber *et al.*, 2004; Lam *et al.*, 2008). Thus nucleosome positioning serves an instructive role for the transcriptional machinery, directing it to the correct regulatory regions and occluding nonfunctional sites (Morse, 2007; Zawadzki *et al.*, 2009).

Given the important role played by promoter NDRs, considerable attention has been devoted to understanding the mechanism by which such regions are formed and maintained. One view posits that a nucleosome positioning code in genomic DNA, based on the

This article was published online ahead of print in MBoC in Press (http://www.molbiolcell.org/cgi/doi/10.1091/mbc.E10-10-0826) on April 20, 2011.

*These authors contributed equally to this work.

†Present address: Department of Developmental Biology, Stanford University School of Medicine, Stanford, CA 94305.

Address correspondence to: James R. Broach (jbroach@princeton.edu); Alexandre V. Morozov (morozov@physics.rutgers.edu).

Abbreviations used: NDR, nucleosome-depleted region; Ribi, ribosomal biogenesis; RP, ribosomal protein; TSS, transcription start site; TTS, transcription termination site.

relative affinities of specific DNA sequences for histone octamers, dictates the location of nucleosomes along the genome (Segal *et al.*, 2006; Field *et al.*, 2008; Kaplan *et al.*, 2009). A countervailing opinion proposes that nucleosome positions derive from the activity of remodeling factors in conjunction with DNA-binding proteins and the transcriptional apparatus, with sequence-specific effects playing a secondary role (Zhang *et al.*, 2009). While large-scale nucleosome positioning maps based on chromatin reconstituted in vitro on genomic DNA have been used to support both positions, the results appear to favor an intermediate viewpoint, in which NDRs are partially reconstituted in vitro but longer-range periodic patterns of nucleosome occupancy are not (Mavrich *et al.*, 2008; Kaplan *et al.*, 2009; Travers *et al.*, 2009; Zhang *et al.*, 2009). Accordingly, chromatin deposition and remodeling factors likely play significant roles in vivo in establishing and maintaining both a fully functional NDR and the periodic organization of nucleosomes extending outward from depleted regions.

Initial positioning of nucleosomes along the genome occurs in the wake of DNA replication and is catalyzed by CAF-1 in conjunction with the H3/H4 histone chaperone Asf1 (Cairns, 2009). After initial deposition, histones in nucleosomes undergo replication- and transcription-independent exchange, both in coding regions and in gene promoters (Dion *et al.*, 2007; Rufiange *et al.*, 2007). The promoter-associated exchange of histone H3, but not exchange within the coding region, substantially depends on Asf1 (Rufiange *et al.*, 2007). This exchange activity likely affects gene expression, since nucleosome removal and transcriptional activation of *PHO5*, *ADY2*, and *ADH2* is delayed in *asf1* mutants (Korber *et al.*, 2006; Adkins *et al.*, 2007; Williams *et al.*, 2008). Thus Asf1 appears to play a significant role in organizing and remodeling chromatin structure in promoter regions.

ATPase-dependent remodeling factors can also contribute to promoter nucleosome organization in vivo. Of the four families of chromatin remodelers in yeast, SWI/SNF and ISW1 family members appear most involved in gene-specific transcriptional regulation and establishing promoter chromatin architecture (Sudarsanam and Winston, 2000; Martens and Winston, 2003; Mellor and Morillon, 2004; Saha *et al.*, 2006). For instance, Whitehouse *et al.* (2007) provide evidence that the ATP-dependent remodeling complex, Isw2, functions to reposition nucleosomes from a subset of genic sequences into adjacent NDRs. Similarly, mutants of *STH1*, the ATPase subunit of RSC, a second complex in the SWI/SNF family, contain excess nucleosomes in the NDRs of a subset of genes located on chromosome III of *Saccharomyces cerevisiae* (Hartley and Madhani, 2009). Mutants of *SNF2*, which encodes the ATPase subunit of yeast Swi/Snf complex, are defective in activation and repression of a subset of genes following environmental stimuli, and exhibit delayed chromatin remodeling at promoters of genes activated under those conditions. This is true for a single locus such as *GAL1* following galactose induction or for a cohort of genes following heat shock or entry into stationary phase (Bryant *et al.*, 2008; Shivaswamy and Iyer, 2008). These observations, along with evidence that SWI/SNF remodelers interact with transcriptional activators (Clapier and Cairns, 2009), suggest that this family of remodelers is recruited to promoters by transcriptional activators, subsequently effecting promoter clearance by evicting or pushing nucleosomes aside.

Despite these recent reports, a clear picture of the interplay between intrinsic affinities of genomic sequences for nucleosome formation and nucleosome remodeler activities has yet to emerge. Do the remodelers act to move nucleosomes to their energetically favored positions on the genome or is the ATPase activity harnessed to reposition nucleosomes to unfavorable positions for purposes of transcriptional regulation? In the former scenario, chromatin remodeling factors facilitate establishing thermodynamic equilibrium, whereas in the latter case, the state of equilibrium would be perturbed, invalidating computational models of nucleosome positioning and energetics based on the thermodynamic assumption. We have recently used a high-throughput sequencing map of nucleosomes assembled in vitro on genomic DNA to develop a thermodynamic model for predicting free energies of nucleosome formation on DNA sequences of arbitrary nucleotide composition (Locke *et al.*, 2010). The model is based on an analogy between nucleosomal arrays and a one-dimensional liquid of finite-size particles in an arbitrary external potential (Percus, 1976). We have used this model to construct a sequence-dependent energy landscape of nucleosome assembly for the yeast genome. We have established that the nature of nucleosome positioning signals in yeast is surprisingly simple—nucleosomes tend to occupy G:C-enriched and A:T-depleted DNA sequences (Chung and Vingron, 2009; Tillo and Hughes, 2009), while periodic dinucleotide distributions and longer motifs typically thought of as primary determinants of nucleosome positioning (Field *et al.*, 2008; Kaplan *et al.*, 2009) play a secondary role in predicting nucleosome occupancies obtained from high-throughput sequencing experiments.

In this report, we have determined nucleosome positions across the yeast genome in wild-type as well as *asf1* and *snf2* mutant strains under both steady-state growth conditions and during substantial transcriptional reprogramming of the cell caused by the change in the carbon source. These data have allowed us to determine that Asf1 and Swi/Snf normally function to move kinetically trapped nucleosomes to their energetically favorable sites in promoters, and that in the absence of these activities subsets of promoter acquire excess nucleosomes that interfere with normal transcriptional activity under steady-state conditions. Moreover, our results demonstrate that transcriptional reprogramming can occur normally in the absence of either of these factors, but that associated chromatin remodeling is either diminished in extent or delayed. These observations suggest that chromatin remodeling follows changes in transcription rather than orchestrating those changes.

RESULTS

Asf1 and Snf2 are required for efficient nucleosome clearance from nucleosome-depleted regions at distinct subsets of promoters

We previously determined all nucleosome positions across the genome in wild-type yeast grown in glycerol, both prior to and immediately after addition of glucose, a carbon upshift that alters expression of approximately one-half of all genes (Zawadzki *et al.*, 2009). We found that most changes in transcription occurred without a corresponding change in promoter nucleosome occupancy, although in the minority of promoters that underwent remodeling, we observed gains in nucleosome occupancy at repressed genes and losses at induced genes. To investigate the contributions of two distinct nucleosome remodeling activities, we examined global nucleosome dynamics in mutants lacking either Snf2, a nucleosome remodeling factor, or Asf1, a histone chaperone; both mutants have altered nucleosome dynamics and positioning at individual gene promoters (Korber *et al.*, 2006; Adkins *et al.*, 2007; Bryant *et al.*, 2008; Shivaswamy *et al.*, 2008; Williams *et al.*, 2008). We examined nucleosome positions in these mutants both under steady-state conditions, which represent the equilibrium positioning state after many generations of growth in a given media, and during massive transcriptional reprogramming caused by a change in carbon source, which exposes the acute phenotype of these mutants during active

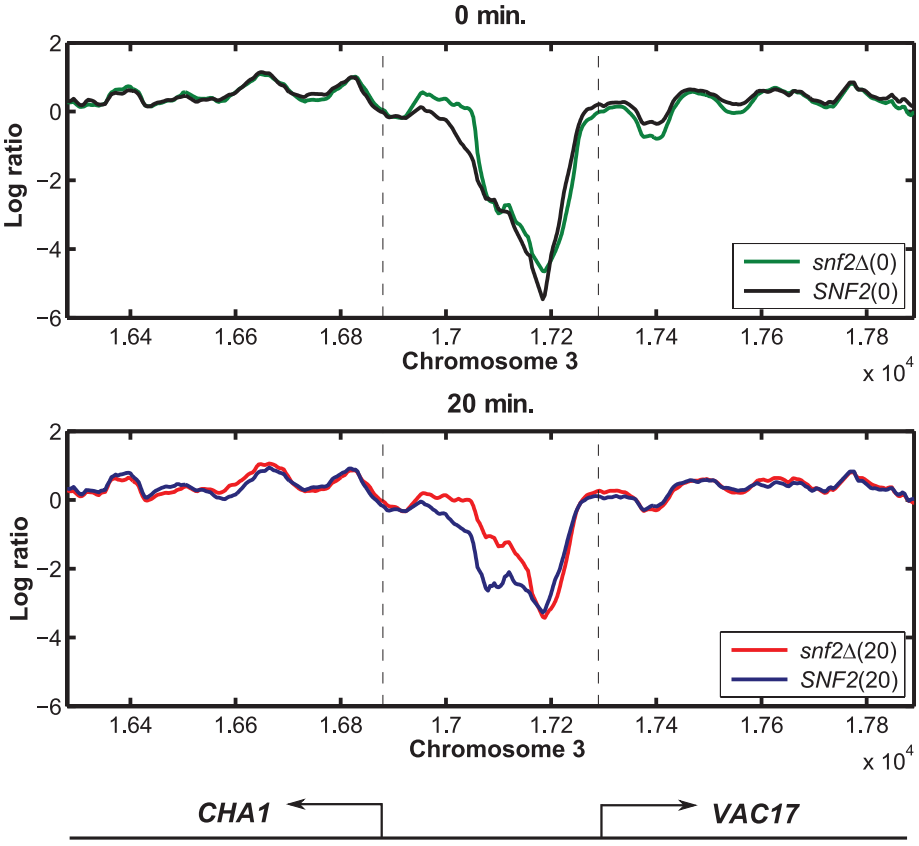

FIGURE 1: Nucleosome occupancy in the *CHA1-VAC17* locus of the *snf2* mutant and wild-type (*SNF2*) cells. Nucleosome occupancy is quantified as the log ratio of intensities from nucleosomal and control DNA hybridized to the tiling array; larger numbers indicate increased nucleosome coverage. Top, steady-state growth in glucose; bottom, 20 min after downshift to glycerol.

nucleosome remodeling. Wild-type yeast and yeast lacking Asf1 were grown in media containing glycerol or glucose (steady-state condition). To the cells grown in glycerol, we then added glucose (carbon upshift). As *snf2* mutants fail to grow with glycerol as the sole carbon source, we examined the reverse transition, initially growing wild-type, *asf1*Δ, and *snf2*Δ yeast in glucose media, and then shifting them to glycerol (carbon downshift).

To determine global nucleosome positions in nucleosome remodeling mutants, we isolated chromatin from wild-type cells as well as *asf1* and *snf2* mutants at steady state and 20 min after carbon downshift (wild-type, *snf2*Δ, *asf1*Δ) or upshift (wild-type, *asf1*Δ). Chromatin was digested by micrococcal nuclease, yielding DNA protected from digestion by inclusion in nucleosomes (Supplemental Figure S1); this nucleosomal DNA was hybridized to Affymetrix tiling arrays covering the entire yeast genome at four to five base pair offset. As an illustrative example, nucleosome occupancy in the *CHA1-VAC17* locus (quantified as the log-intensity ratio between nucleosomal and control DNA hybridized to the tiling array) is shown in Figure 1.

When we examined nucleosome positioning in *asf1* and *snf2* mutants grown at steady state in either glycerol or glucose, we found that distinct subsets of promoters were altered in the mutants relative to wild-type (Figures 2 and S2A). While the promoter nucleosome occupancy patterns of a majority of genes in both *snf2* or *asf1* mutants were identical to those in wild-type, 20% of genes in glucose-grown *snf2* (900/4532), 43% of genes in glucose-grown *asf1* (1948/4532), and 25% of genes in glycerol-grown *asf1* (1051/4532) contained an excess of nucleosomes in their promoters; few promoters in either mutant had decreased nucleosome levels. Deleting *SNF2* or *ASF1* affects promoters of distinct gene subsets with only limited overlap under glucose growth conditions (540 genes in common). The set of genes affected by *SNF2* deletion is significantly enriched for TATA box–containing promoters (Huisinga and Pugh, 2004) (222/900 genes, $p = 5.9 \times 10^{-10}$) and for genes at which Snf2 has been shown to bind in vivo by prior chromatin immunoprecipitation experiments ($p = 0.003$) (Shivaswamy and Iyer, 2008). In contrast, promoters with additional nucleosomes in the *asf1* mutant are depleted of TATA boxes, both in glucose (290/1948 genes, $p = 2.1 \times 10^{-5}$) and glycerol (111/1051 genes, $p < 10^{-10}$). Previous studies have shown that NDRs exist not only over promoters but also over the transcription termination sites (TTS) of most genes (Mavrich *et al.*, 2008; Kaplan *et al.*, 2009). Both *snf2* and *asf1* mutants display an excess of nucleosomes over the TTS in largely distinct subsets of genes (Figure S3), but excess TTS nucleosomes are not correlated with excess promoter nucleosomes in either mutant. The positions of nucleosomes over coding regions were essentially unchanged in the mutants. In sum, we conclude that both the histone chaperone Asf1 and the Swi/Snf complex act under steady-state conditions to remove, or prevent the deposition of, nucleosomes at specific and largely nonoverlapping sets of promoter and terminator regions.

Mutation of either *SNF2* or *ASF1* leads to excess promoter nucleosomes at distinct locations and consequently at distinct sets of sequences. As Snf2 is an ATPase that expends energy when remodeling or removing nucleosomes, but Asf1 is not, we wondered if those sequences that gained nucleosomes in the *snf2* mutant were intrinsically more favorable for nucleosome assembly than those in the *asf1* mutant. Accordingly, we compared the energy cost associated with excess nucleosomes present at steady state in both mutants. Our biophysical model of nucleosome energetics accounts for intrinsic histone–DNA interactions and for steric exclusion between neighboring nucleosomes, and thus captures nucleosome positioning preferences in the absence of external factors (Locke *et al.*, 2010). We calculated the average sequence-dependent free energy of nucleosome formation in vitro for each promoter in the yeast genome, and compared that to the extent of excess nucleosome occupancy in that promoter (Figures 3 and S2B). Surprisingly, excess nucleosomes in *snf2* cells tend to occur at promoters with a high energy cost of nucleosome assembly (Figure 3A; $p < 10^{-10}$). A similar correlation holds for *asf1*, both in glucose (Figure S2B; $p < 10^{-10}$) and glycerol (Figure 3B; $p < 10^{-10}$). Thus Snf2 and Asf1 function to remove nucleosomes from those promoters on which it is most difficult to assemble nucleosomes in vitro. We conclude that under steady-state conditions both activities move nucleosomes to more thermodynamically stable positions on the genome, which suggests that excess nucleosomes are kinetically trapped at their inappropriate sites. It appears that Snf2 and Asf1 mediate transition toward

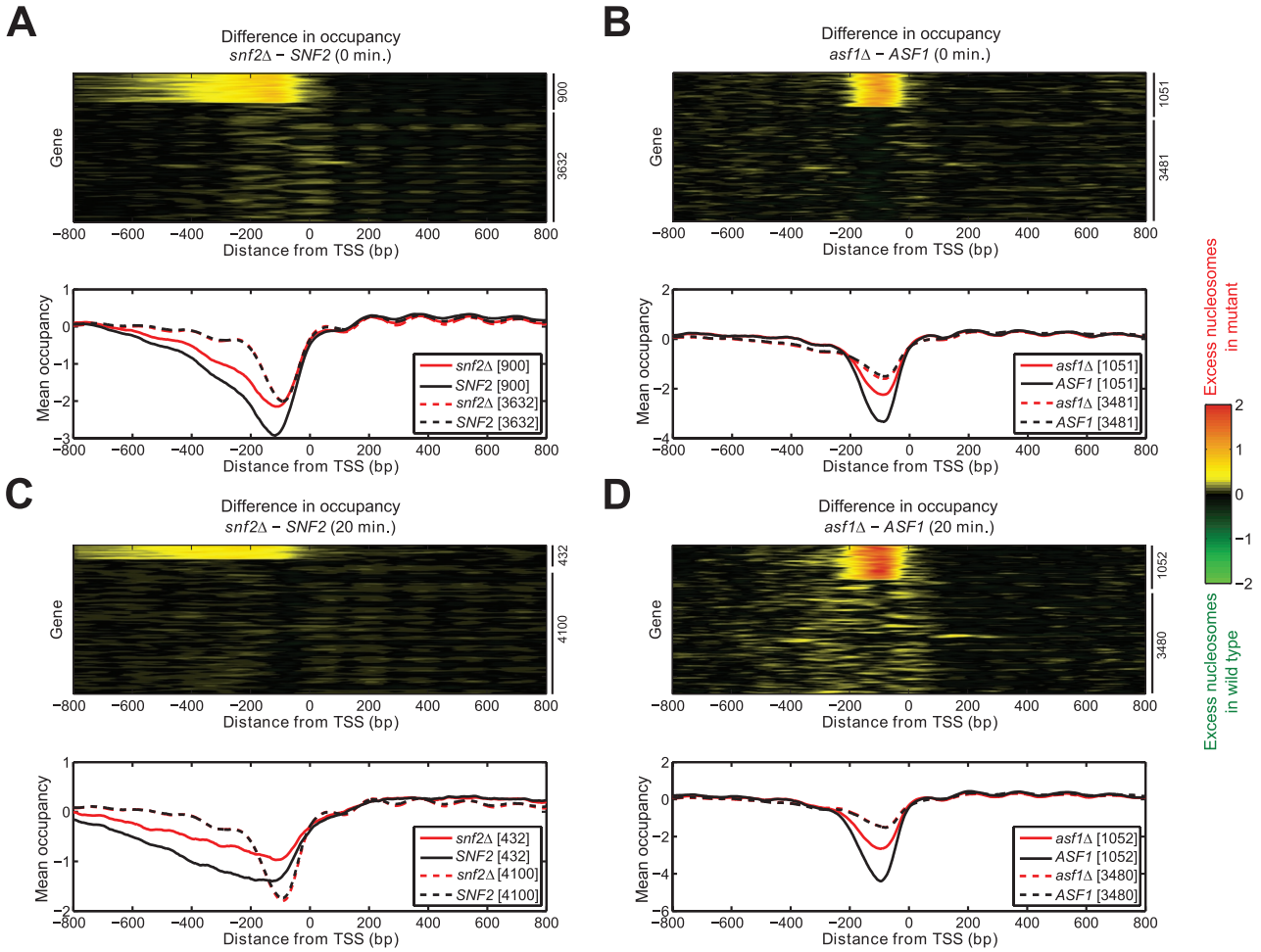

FIGURE 2: *snf2* and *asf1* mutants contain excess promoter nucleosomes. (A) Top, nucleosome occupancy (quantified as the log ratio of intensities from nucleosomal and control DNA hybridized to the tiling array) in the wild-type strain grown in glucose is subtracted from the occupancy in the *snf2* mutant strain grown in glucose; positive values indicate excess nucleosomes in the mutant relative to wild-type (see scale on right). Nucleosome occupancy difference as a function of position is shown 800 base pairs upstream and downstream of the transcription start site (TSS) (Nagalakshmi *et al.*, 2008) for 4532 genes. The occupancy difference is clustered into two groups using K-means. The upper cluster shows excess nucleosomes in the *snf2* mutant. (B) Top, *asf1* mutant grown in glycerol vs. wild-type grown in glycerol. (C) Top, *snf2* mutant 20 min after downshift to glycerol vs. downshifted wild-type. (D) Top, *asf1* mutant 20 min after upshift to glucose vs. upshifted wild-type. (A–D) Bottom, average nucleosome occupancy in the two clusters for each mutant–wild-type combination. Solid lines correspond to the cluster with excess nucleosomes in the mutant strain.

thermodynamic equilibrium, lowering the total free energy of nucleosomal arrays.

Excess nucleosomes in *snf2*, but not *asf1*, suppress transcription

We were interested in determining the influence on transcription of the excess promoter nucleosomes in *snf2* and *asf1* yeast strains. We examined global mRNA levels in both the *snf2* and *asf1* mutants relative to wild-type, both before and after changing the carbon source (Figures 4 and S2C). In Figure 4A, we have organized all yeast genes by the difference in expression between wild-type and *snf2*. As evident from the corresponding differential promoter nucleosome occupancy, the reduction in expression in *snf2* mutants is highly correlated with the presence of excess promoter nucleosomes ($r = 0.83$, $p < 10^{-10}$). Moreover, in *snf2* mutants, differences in nucleosome occupancy appear exclusively in genes with reduced expression, and not in those genes showing increased expression, suggesting that increased expression of genes in the mutant is most likely a secondary effect of the loss of Snf2 function. In contrast, the correlation between expression changes in *asf1* mutants and excess promoter nucleosomes is substantially lower. As seen in Figures 4B and S2C, excess nucleosomes are present at gene promoters with increased, normal, and reduced expression, and the correlation between reduced expression and excess nucleosomes is much weaker for cells grown in glycerol ($r = 0.52$, $p = 2.77 \times 10^{-5}$) or glucose ($r = 0.19$, $p = 0.23$). The situation is qualitatively similar 20 min after the carbon source change (Figure 4, C and D). Thus, while excess nucleosomes in the *snf2* mutant generally suppress gene expression, the effect in the *asf1* mutant is significantly less dramatic.

We examined the relationship between additional promoter nucleosomes and transcription factor binding motifs in yeast cells lacking *SNF2* or *ASF1*. We have previously identified sequence motifs corresponding to transcription factor binding sites that are enriched in promoters of genes either up-regulated or down-regulated by glucose addition (Zaman *et al.*, 2009). Further, we have found that in wild-type cells these glucose motifs tend to be depleted of nucleosomes at promoters regulated by glucose upshift, suggesting that physiological transcription factor binding sites are

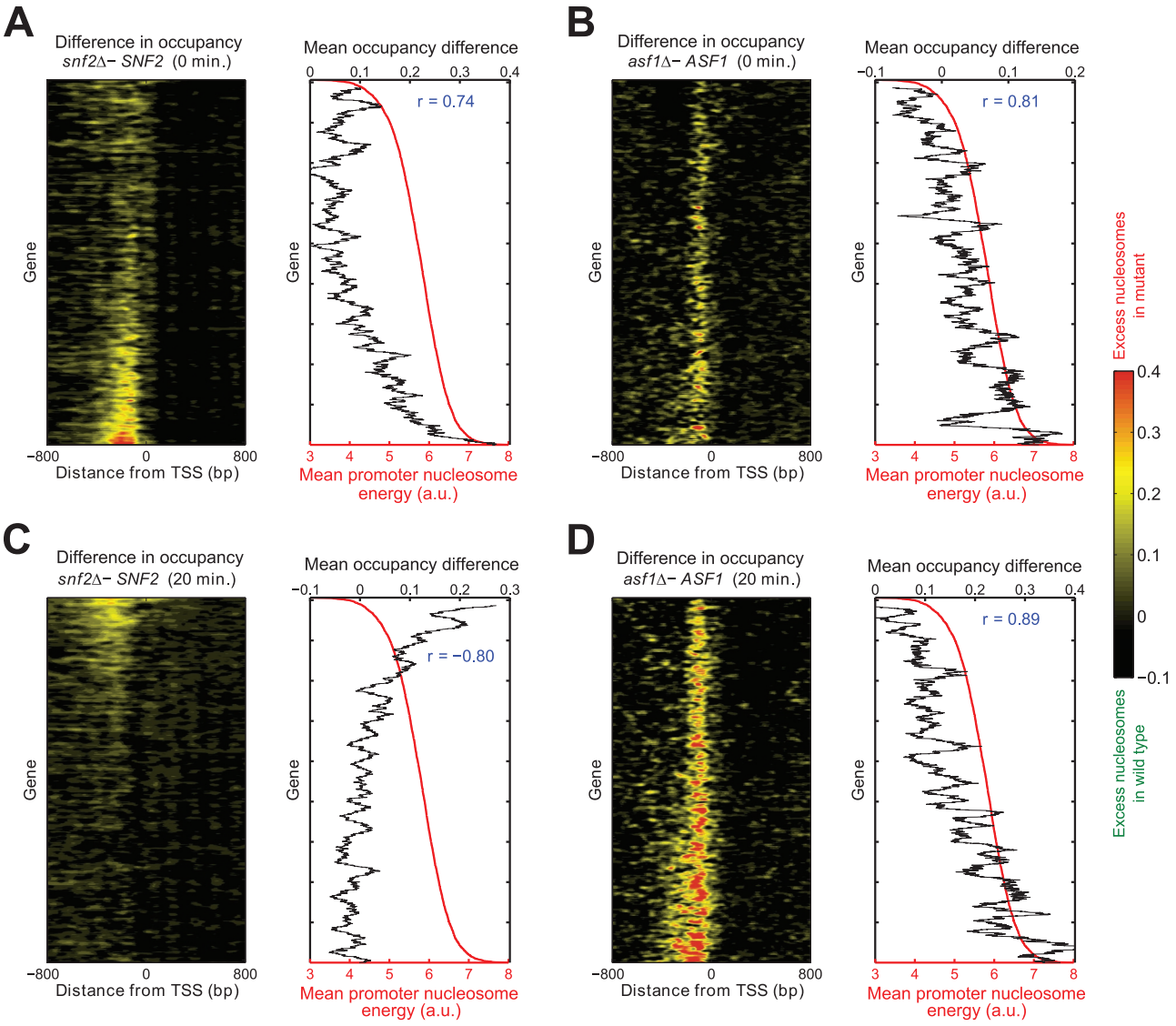

FIGURE 3: Energetics of excess promoter nucleosomes. The difference in nucleosome occupancy between mutant and wild-type is computed for all gene promoters as in Figure 2, and the genes are sorted by the average free energy of nucleosome formation in promoters. (A) Steady-state *snf2* mutant and wild-type in glucose. (B) Steady-state *asf1* mutant and wild-type in glycerol. (C) *snf2* mutant and wild-type 20 min after glucose-to-glycerol downshift. (D) *asf1* mutant and wild-type 20 min after glycerol-to-glucose upshift. The average free energy is computed as the mean of the nucleosome formation energies in the [−400 base pairs, −100 base pairs] window upstream of the TSS (each position in the window is taken as a starting base pair of a 147–base pair nucleosome core particle). The free energy at each position is given by the model defined in Eq. (3) (see *Materials and Methods*). Excess promoter nucleosomes in the deletion strains tend to reside on energetically less (A, B, and D) or more (C) favorable sequences. On the right, the red lines show the mean nucleosome energy over the promoter (more positive energy values indicate that nucleosomes reside on relatively less favorable DNA sequences). The black lines are the net differences in nucleosome occupancy between the mutant and the wild-type across each promoter, smoothed with a 100-gene moving average; larger values indicate more net excess nucleosomes in mutants. In each panel, the Pearson correlation coefficient r is shown for the smoothed occupancy differences. The p values (computed using a two-tailed Student's *t* test) for the unsmoothed occupancy differences are $< 10^{-10}$ in all cases; the Pearson correlation coefficients are 0.28, 0.15, −0.27, and 0.25 for A, B, C, and D, respectively.

often constitutively accessible (Zawadzki *et al.*, 2009). When we examine the steady-state nucleosome occupancy of these motifs in *snf2* and *asf1* mutants, we find that they are, on average, more occluded by nucleosomes in the *snf2* and *asf1* mutants grown in glucose compared with wild-type cells (gray bars in Figure 5, A and C), but not in the *asf1* mutant grown in glycerol (gray bars in Figure 5B). The genes most significantly upregulated in response to glucose upshift are those involved in the production of ribosomes, and the promoters of these genes are strongly enriched in PAC-, RRPE-, Rap1-, and Mbp1-binding sites (Zaman *et al.*, 2009); those sites are particularly occluded by nucleosomes in the *snf2* mutant. Further, the genes involved in the production of ribosomes are on average expressed at a significantly lower level in *snf2* than in wild-type cells (Figure S4). This suggests that in glucose both Snf2 and Asf1 function to expose the corresponding binding sites to active transcription factors.

As shown in Figure S5, transcription factor binding sites in most promoters tend to lie between 50 and 150 base pairs upstream of

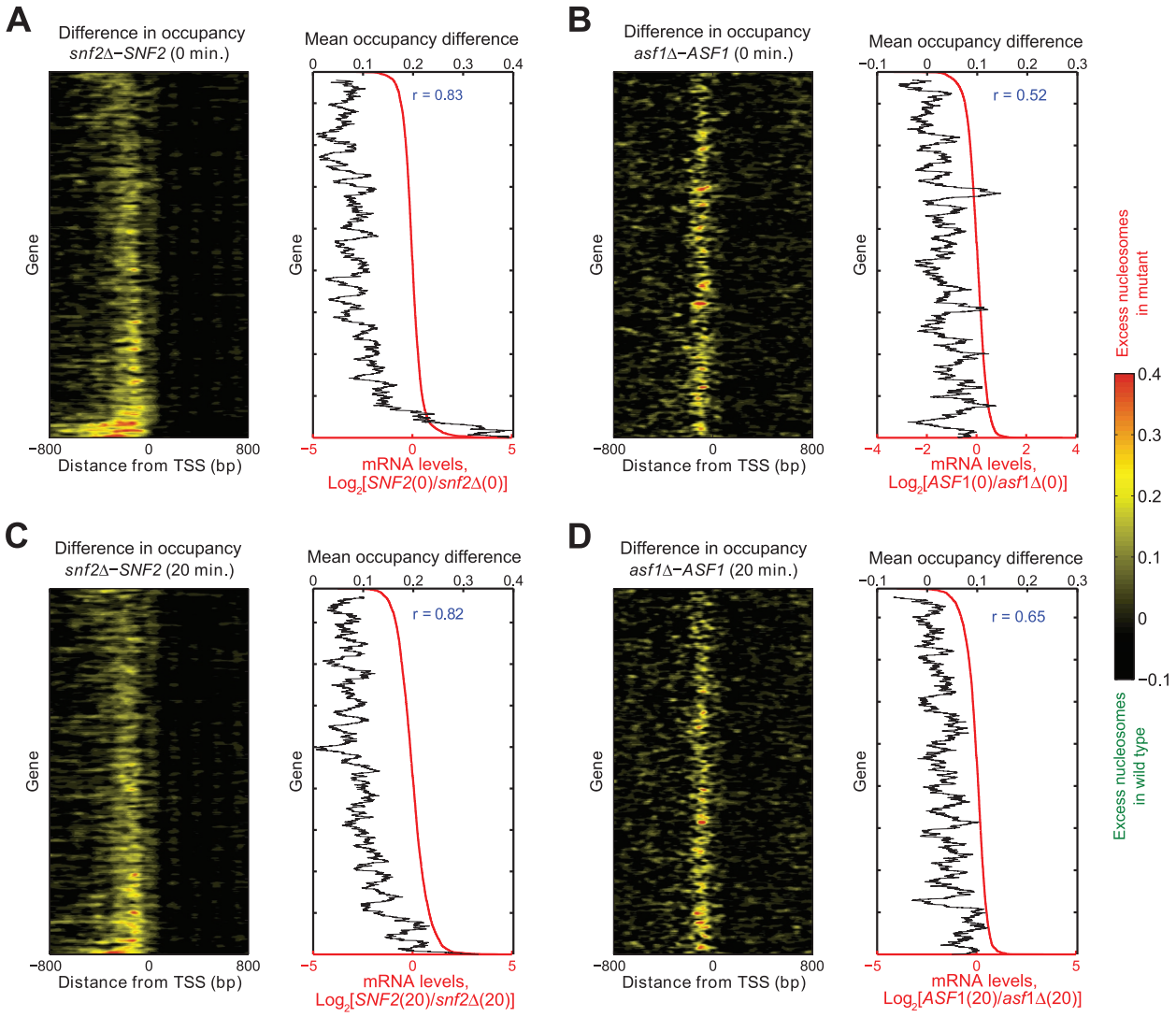

FIGURE 4: Excess promoter nucleosomes and transcription. (A) Steady-state *snf2* mutant and wild-type in glucose. (B) Steady-state *asf1* mutant and wild-type in glycerol. (C) *snf2* mutant and wild-type 20 min after glucose-to-glycerol downshift. (D) *asf1* mutant and wild-type 20 min after glycerol-to-glucose upshift. (A–D, left panels) The difference in nucleosome occupancy between mutant and wild-type is computed for each gene promoter, as in Figure 2, and the genes are sorted by the difference in mRNA expression levels shown as red lines on the corresponding right panel in (A–D). Positive values indicate less gene expression in mutant. As in Figure 3, the black lines show the difference in net promoter nucleosome occupancy between mutants and corresponding wild-types. In each panel, the Pearson correlation coefficient r is shown for the smoothed occupancy differences. The p values (computed using a two-tailed Student's *t* test) for the unsmoothed occupancy differences are $< 10^{-10}$ (A), 2.77×10^{-5} (B), $< 10^{-10}$ (C), 1.01×10^{-5} (D). The Pearson correlation coefficients for unsmoothed data are 0.19, 0.05, 0.15, and 0.07 for A, B, C, and D, respectively.

the TSS. However, excess nucleosomes found in *snf2* mutants occur disproportionately in the promoters of TATA box–containing genes, which tend to have larger NDRs (Mavrich *et al.*, 2008; Zawadzki *et al.*, 2009); consequently, promoters with excess nucleosomes in the *snf2* mutant are enriched for transcription factor binding sites residing further upstream (Figure S5, A and B). There is no enrichment for distant transcription factor binding sites in *asf1* promoters with excess nucleosomes (Figure S5, C and D).

Deletion of *Asf1* predominantly affects promoters with low nucleosome exchange rate

Histone exchange can take place in the absence of DNA replication, with exchange at gene promoters occurring more rapidly than in coding regions (Dion *et al.*, 2007; Rufiange *et al.*, 2007). The histone exchanges rates of promoters vary widely for reasons that are not well understood, but seem to be largely independent of the transcription rate of their corresponding genes. We find that gene promoters that contain additional nucleosomes in the *asf1* mutant grown in glycerol tend to have low histone exchange rates, as measured by either previous study (Figure 6). This correlation is also observed in the *asf1* mutant grown in glucose, but absent in the *snf2* mutant (unpublished data). These results are consistent with our observation that excess nucleosomes in *asf1*Δ cells reside on sequences that are energetically less favorable for nucleosome formation. Those nucleosomes that are relatively rapidly exchanged might be expected to reach their thermodynamically preferred positions by repeated removal and redeposition. On the other hand, slowly exchanging nucleosomes might tend to remain trapped at

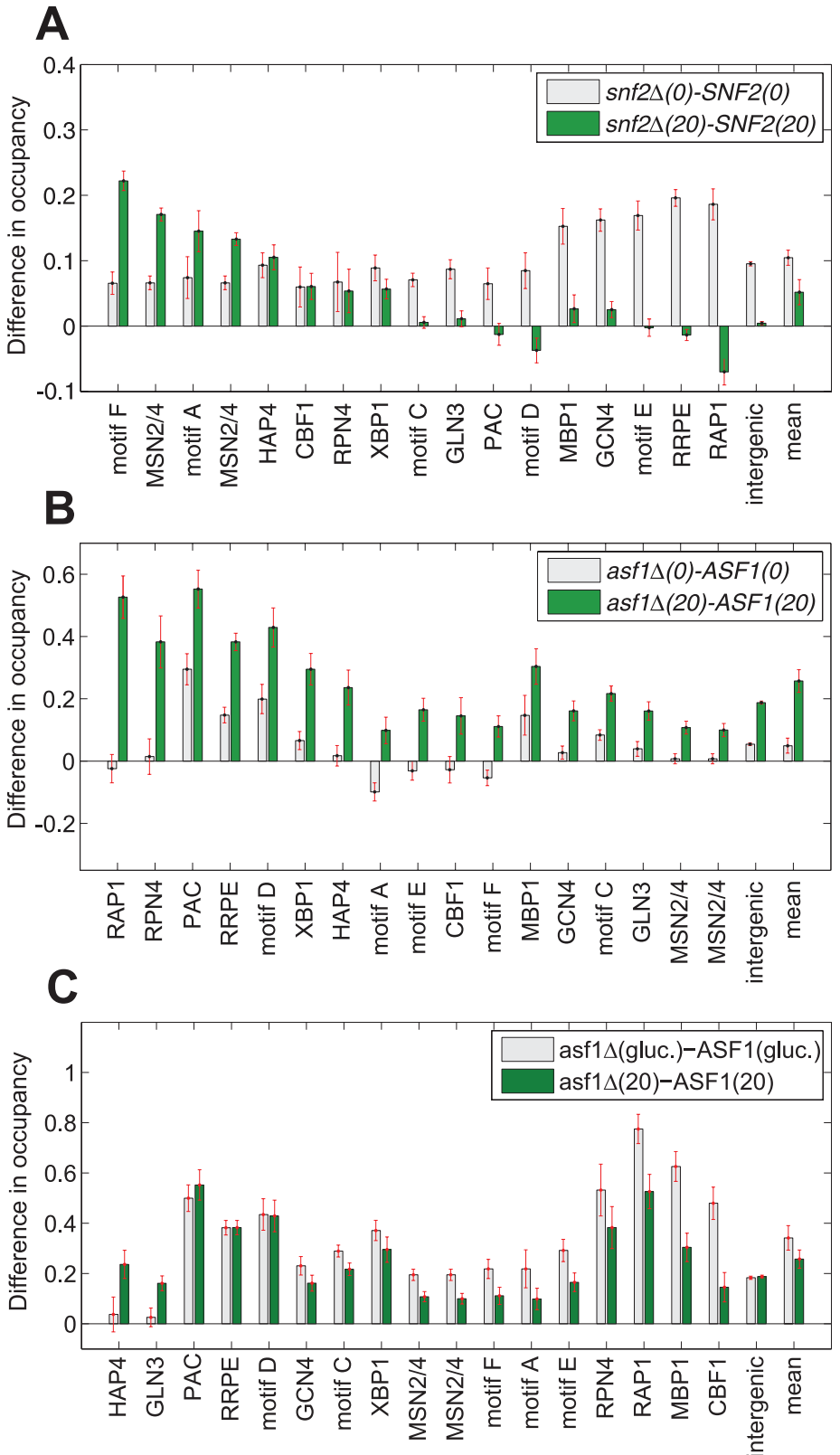

FIGURE 5: Nucleosome occlusion of transcription factor motifs in the *snf2* mutant (A) and the *asf1* mutant (B, C) relative to wild-type. Differences in the average nucleosome occupancy (quantified as log intensity) between the mutant and the wild-type were computed for a set of glucose-related transcription factor motifs from our previous studies (Zaman *et al.*, 2009; Zawadzki *et al.*, 2009). In (A), the nucleosome occupancy differences between the *snf2* mutant and the wild-type are plotted for steady-state growth in glucose (gray bars) and 20 min after the downshift to glycerol (green bars). In (B), the occupancy differences between the *asf1* mutant and the wild-type are plotted for steady-state growth in glycerol (gray bars) and 20 min after the upshift to glucose (green bars). In (C), the occupancy differences between the *asf1* mutant and the wild-type at steady-state growth in glucose (gray bars) are compared with the corresponding differences 20 min after the upshift from glycerol to glucose (green bars). Shown are the average and the SE of the nucleosome occupancy difference for each binding motif (the occupancy of a single binding site is defined as the average occupancy of all base pairs in that site; occupancies of all sites of a given type are used to compute the average and the SE for each binding motif). The bar labeled "intergenic" indicates changes in the nucleosome occupancy over entire promoters (defined as intergenic regions upstream of each TSS, between 100 and 800 base pairs in length), and the bar labeled "mean" refers to the net change in nucleosome occupancy over all types of binding sites. Transcription factor motifs are as follows: Cbf1, [CGT]CA[CG]GTG[AG][AC]; Gcn4, TGACT[ACT]A; Gln3, [ACT]GATAAG[ACG]; Hap4, [ACG]CCA[AC]TCA; Mbp1, T.[AT]CGCGT[ACT]; Msn2/4, [ACG][AG][ACT].GGGG or CCCCT[AGT]; PAC, CTCATC[GT]C; Rap1, A[CT]CC.ACA[CT]; Rpn4, TT[CT]GCCACC; RRPE (motif B), [ACG]AAANTTTT; Xbp1, [CT][CT]TCG[AC]G[AG][CGT]. Unassigned motifs are defined as (Zawadzki *et al.*, 2009): (A) CGC[AG]C[CT]C[AT]; (C) [AGT][AT][AT]AAGGG; (D) GATCN$_3$TGA[AG]; (E) [CGT]TA[AT]ACGA.; (F) [CGT]CCGN$_5$CC[ACG].

unfavorable positions, and thus be more dependent on Asf1 activity to reach thermodynamic equilibrium. Thus the correlation between excess promoter nucleosomes in *asf1* mutants and slow histone exchange is consistent with the requirement for Asf1 to establish thermodynamic equilibrium by depositing nucleosomes at their energetically more favorable sites.

Snf2 and Asf1 act on specific promoters during transcriptional reprogramming

During steady-state growth on glycerol, ~25% of yeast genes have excess nucleosome density over their 5′ NDRs in *asf1* mutants versus wild-type cells (Figure 2B). Following transition to glucose, the excess nucleosome density is lost over many promoters but additional promoters gain nucleosomes, such that ~25% of all gene promoters still contain excess nucleosome density (Figure 2D). A statistically significant number of genes (422) carry excess nucleosomes under both conditions ($p < 10^{-10}$). In both conditions, excess nucleosomes reside on energetically less favorable sites (Figure 3, B and D), indicating that Asf1

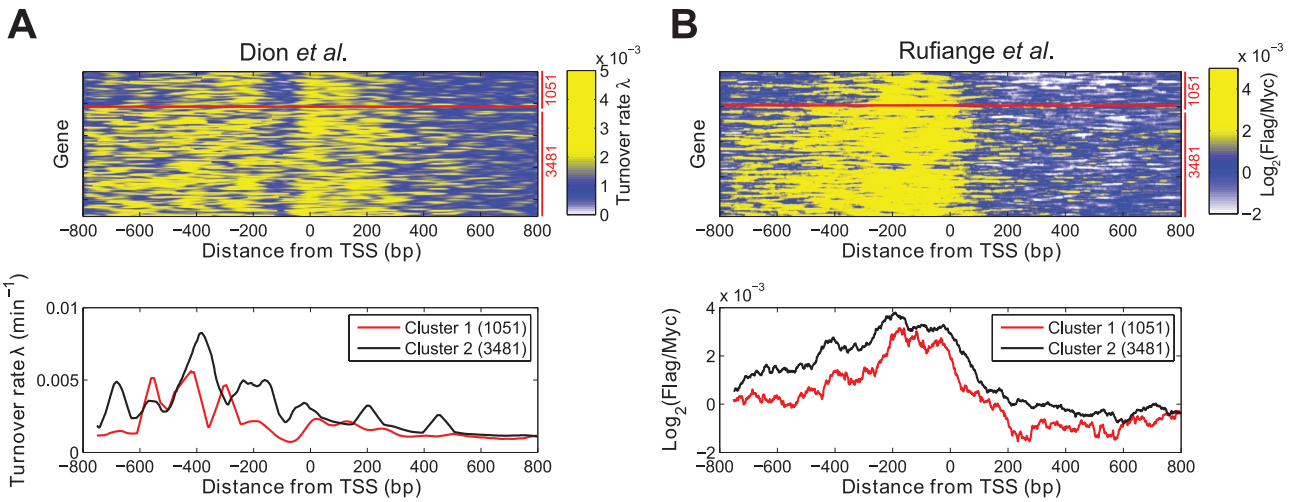

FIGURE 6: Promoters with slow histone exchange rates have excess nucleosomes in *asf1*Δ. (A) Top, frequency of H3 histone turnover events measured by the rate parameter λ (Dion *et al.*, 2007) is sorted into two steady-state clusters from Figure 2B; larger λ values indicate faster histone turnover. In the histone turnover study, yeast cells were grown in the YP + 2% galactose medium. To reduce the noise, we applied a Gaussian low-pass filter with σ = 50 base pairs. The horizontal red line is the boundary between the clusters. (A) Bottom, the frequency of histone turnover events averaged over the two clusters from Figure 2B. (B) Top, histone H3 exchange rate $\log_2$(Flag-H3/Myc-H3) (Rufiange *et al.*, 2007) is sorted and smoothed with a Gaussian low-pass filter as in (A, Top); larger values indicate faster histone exchange. Yeast cells were grown in the YP + 2% galactose medium. (B) Bottom, histone H3 exchange rate averaged over the two clusters from Figure 2B.

assists in redistributing kinetically trapped nucleosomes both before and during transcriptional reprogramming. A similar situation is observed for NDRs located at the 3′ ends of genes (Figure S3, B and D).

The NDRs of promoters of ~20% of genes in the *snf2* mutant grown on glucose contain excess nucleosome density (Figure 2A). Twenty minutes after downshift to growth on glycerol, the excess nucleosome density in most of these promoters is cleared, although a significant number retain their excess nucleosomes (294 of the initial 900, $p < 10^{-10}$) and additional promoters (138) acquire excess nucleosomes (Figure 2C). Remarkably, in the *snf2* mutant excess nucleosomes reside on energetically less favorable sites before the downshift (Figure 3A), whereas the excess nucleosomes occupy energetically more favorable sites after the downshift (Figure 3C). This would suggest that, in contrast to its role during steady-state growth on glucose, Snf2 activity upon glucose downshift is required to extract nucleosomes from energetically favorable sites, presumably using ATP hydrolysis to reposition nucleosomes to less favorable sites. This behavior is not observed with Asf1, which lacks ATPase activity and thus cannot expend energy to reposition nucleosomes to sites with higher free energies of nucleosome formation.

asf1 and *snf2* mutants exhibit delayed nucleosome repositioning during transcriptional reprogramming

Large-scale transcriptional reprogramming follows an upshift from glycerol to glucose, during which approximately one-half of all yeast genes exhibit a significant change in expression levels (Zaman *et al.*, 2009) (Figure S6A). We previously showed that only a minority of genes undergo promoter nucleosome restructuring under this upshift (Zawadzki *et al.*, 2009). Consistent with this previous study, we find that in wild-type cells undergoing transcriptional reprogramming there is only a weak correlation between the change in mRNA expression of a gene and a *t* statistic metric of promoter nucleosome remodeling, either for the upshift from glycerol to glucose (Figure 7A; r = −0.28) or the downshift from glucose to glycerol (Figure 7B; r = −0.19). Thus, during two examples of substantial transcriptional reprogramming, chromatin remodeling is associated with, but not the primary mediator of, transcriptional changes.

To understand the acute phenotype of *snf2* and *asf1* mutants during nucleosome remodeling associated with transcriptional reprogramming, we measured global nucleosome positions and gene expression in mutant strains 20 min after their respective carbon source shifts, and compared their responses to wild-type. To compare mutant and wild-type nucleosome remodeling during the shift, we quantified nucleosome remodeling at each promoter as the *t* statistic of the difference between nucleosome occupancies before and after carbon source shift, then compared the *t* statistic scores between wild-type and mutant yeast (Figure 7, C and D). For the *snf2* mutant (Figure 7D), we observed a high correlation between the promoter nucleosome changes in the *snf2* strain and the wild-type strain (r = 0.69), demonstrating that most of the nucleosome remodeling that takes place in wild-type under this transition also occurs in the absence of the Snf2 function. However, the slope of the linear fit line in the correlation plot is below the diagonal, suggesting that, while essentially the same nucleosome occupancy changes occur in the mutant as in the wild-type, on average they occur either less extensively or more slowly in the mutant. As shown in Figure 7C, similar results are observed in the *asf1* mutant grown in glycerol: the nucleosome occupancy changes in the mutant correlate well with those in the wild-type (r = 0.59), but the changes are either less extensive or delayed in the mutant. We find only a limited correlation between changes in gene expression and changes in promoter nucleosome occupancy for both mutants, similar to wild-type cells (Figure 7, E and F). Thus, in the mutants as in the wild-type, nucleosome remodeling is not a major component of transcriptional reprogramming.

The delayed (or less extensive) nucleosome remodeling in the mutants relative to wild-type cells is mirrored by a delay in exposing transcription factor binding sites. We compared the change in nucleosome occupancy over glucose-related transcription factor

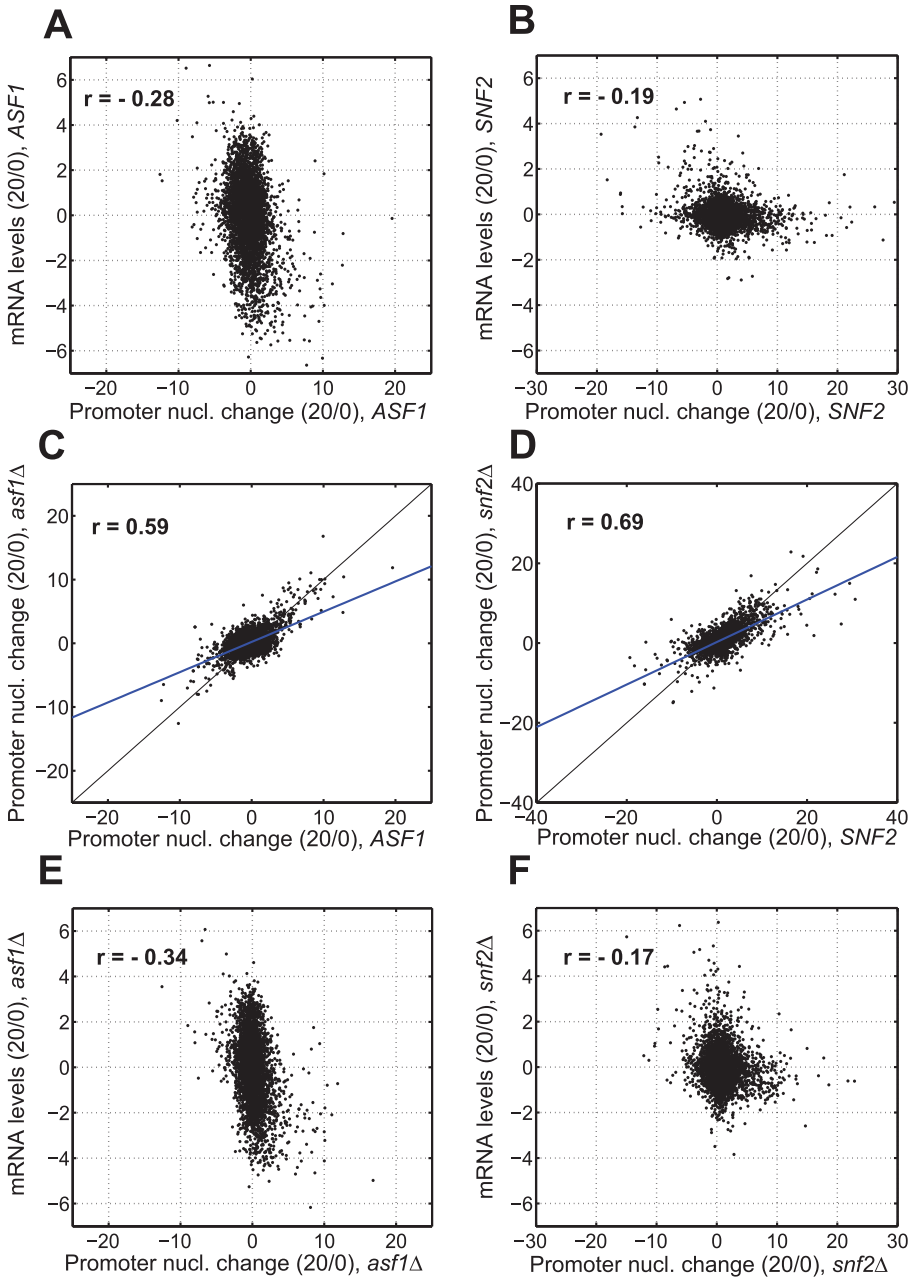

FIGURE 7: Transcriptional changes and nucleosome remodeling. (A) Relationship between changes in mRNA expression levels and the extent of nucleosome remodeling in wild-type cells upshifted from glycerol to glucose. For each gene, we plotted the *t* statistic measure of the change in wild-type promoter nucleosome occupancy on the *x*-axis and the corresponding $\log_2$ ratio of mRNA expression levels on the *y*-axis. The *t* statistic for each promoter is defined as the normalized difference between promoter nucleosome occupancies at 20 and 0 min: $t = (\bar{O}_{20} - \bar{O}_0) \Big/ \sqrt{(S^2_{O_{20}} + S^2_{O_0})N^{-1}}$, where $\bar{O}_0$ ($\bar{O}_{20}$) and $S^2_{O_0}$ ($S^2_{O_{20}}$) are the mean and the variance of *N* nucleosome occupancies averaged in the [−700 base pairs, 0 base pairs] window upstream of each TSS at 0 and 20 min, respectively. (B) Same as (A), for the downshift from glucose to glycerol in wild-type cells. (C) Scatter plot showing the correlation between nucleosome remodeling in the *asf1* mutant and the wild-type upon upshift from glycerol to glucose. For each gene we plot on the *x*-axis, the *t* statistics measure of the change in wild-type promoter nucleosome occupancy 20 min after the upshift relative to that before the upshift, and on the *y*-axis, the corresponding *t* statistics for the *asf1* mutant. (D) Same as (C), for the wild-type and the *snf2* mutant downshifted from glucose to glycerol. (E) Same as (A), for the *asf1* mutant upshifted from glycerol to glucose. (F) Same as (B), for the *snf2* mutant downshifted from glucose to glycerol.

motifs (Zaman *et al.*, 2009) between wild-type and mutant yeast during their respective carbon shifts. As is evident from Figure 5B, the additional occlusion of transcription factor binding motifs in the *asf1* mutant relative to wild-type during steady-state growth on glycerol becomes much more pronounced at 20 min following glucose upshift. In fact, the degree of occlusion becomes very similar to that observed for the *asf1* mutant and wild-type grown in glucose under steady-state conditions (Figure 5C). This indicates that promoter nucleosomes equilibrate into their new steady-state configuration essentially within 20 min following transition to growth on glucose. The increased exposure of motifs in the wild-type versus the *asf1* mutant results from the fact that wild-type cells tend to remove nucleosomes from transcription factor motifs following transition to glucose, whereas the *asf1* mutant fails to do so, either at short times following the transition or upon reaching steady state (Figure S7A). For instance, Rap1- and Rpn4-binding motifs become substantially exposed in wild-type cells during transcription reprogramming but fail to do so in *asf1* mutants. Thus Asf1 facilitates removal of nucleosomes from a large number of transcription factor binding sites upon carbon source transition.

Yeast lacking *SNF2* have excess nucleosomes occluding active transcription factor binding motifs both at steady state and during nucleosome remodeling driven by transcriptional reprogramming. During steady-state growth on glucose, glucose-activated transcription factor binding sites are more occluded in the *snf2* mutant than in the wild-type (gray bars in Figure 5A); notably, the PAC-, RRPE-, and Rap1-binding motifs, which drive expression of the highly transcribed ribosomal biogenesis (Ribi) and ribosomal protein (RP) genes during growth on glucose (Zaman *et al.*, 2009), are on average significantly more occluded by nucleosomes in the *snf2* mutant than in the wild-type. Following the carbon source downshift, Ribi and RP genes are down-regulated in both *snf2*Δ and wild-type yeast, and the occupancy of the corresponding transcription factor binding sites becomes more equal (Figure 5A, green bars). However, stress response genes are induced after the downshift and, correspondingly, the Msn2/4-binding sites, which drive the stress response genes, become more exposed in the wild-type than in the *snf2* mutant. These results are consistent with the hypothesis that Snf2 functions to stimulate exposure of the binding motifs for those transcription factors that are most active in the cell. Thus Snf2 appears to work in concert with different transcription factors, facilitating access to their cognate binding sites only when needed.

Remarkably, the differential exposure of transcription factor binding sites in the mutants versus wild-type during metabolic

upshift or downshift does not affect transcriptional reprogramming. For instance, during carbon upshift, Rap1-binding motifs become exposed in the wild-type, consistent with the induced expression of Rap1-regulated RP genes (Figure S7B). While, as noted above, this uncovering of the Rap1-binding motifs does not occur in the *asf1* mutant (Figure S7B), induction of RP gene expression happens at the same rate in the mutant as in the wild-type strain (Figure S6A). Similarly, while Msn2/4-binding motifs become more exposed in the wild-type than in the *snf2* mutant during carbon downshift (Figure S7E), induction of stress response genes occurs similarly in both the *snf2* mutant and the wild-type (Figure S6A). Likewise, while Rap1 motifs become more occluded in the wild-type than in the *snf2* mutant during carbon downshift (Figure S7F), RP gene expression is repressed at least as strongly in the *snf2* mutant as in the wild-type yeast (Figure S6A). Moreover, Ribi gene repression is substantially greater in the *snf2* mutant than in the wild-type during carbon downshift, even though both strains exhibit very similar changes in RRPE and PAC motif occlusion (Figures S7F and S6B). Thus transcriptional reprogramming does not strongly depend on chromatin remodeling promoted by either Asf1 or Swi/Snf.

DISCUSSION

We have examined global positioning of nucleosomes in yeast cells in strains lacking either the Swi/Snf ATP-dependent chromatin remodeling activity or the histone H3/H4 chaperone Asf1. We find excess nucleosome density over promoters and TTS of distinct subsets of genes in both mutant strains. These results suggest that a primary function of both Swi/Snf and Asf1 is to promote nucleosome depletion of the regulatory regions upstream and downstream of genes. We note that Asf1 also serves as a specificity factor for the H3K56 acetyl transferase, Rtt109, and that *asf1* mutants are therefore deficient in H3K56 acetylation (Driscoll *et al.*, 2007; Han *et al.*, 2007). While it is possible that the effects we observe with *asf1* are a result of reduced histone acetylation, a direct participation of Asf1 in nucleosome remodeling seems likely. This would be consistent with previous studies on the effect of Swi/Snf and Asf1 on chromatin structure of several yeast genes. For instance, both Swi/Snf and Asf1 are required to remove nucleosomes from URS2 during G1-specific cell cycle activation of *HO* gene expression (Gkikopoulos *et al.*, 2009; Takahata *et al.*, 2009). While a few exceptions have been noted, such as the apparent role of Asf1 in repressing HTA/HTB gene expression by increasing nucleosome density over their promoters (Fillingham *et al.*, 2009), our results indicate that during steady-state growth both Snf2 and Asf1 function predominantly to clear nucleosomes from promoters.

We note that excess nucleosome density is not simply due to the addition of a discrete nucleosome in mutant cells—rather, it reflects a fractional increase in the average nucleosome occupancy over the affected promoters in the mutant population as a whole. That is, a greater fraction of cells in wild-type than in mutant are depleted of nucleosomes over the affected areas. Our analysis of the genes influenced by these activities and the effects of these mutants on repositioning of nucleosomes following transcriptional reprogramming allows us to draw conclusions regarding the biological roles of these chromatin-modifying factors.

Remodeling factors remove kinetically trapped nucleosomes from NDRs

Our studies revealed that both *asf1* and *snf2* mutants accumulate excess nucleosome density under steady-state growth conditions, predominantly over those promoters that are least energetically favorable for nucleosome assembly in vitro, suggesting that both Asf1 and Swi/Snf function to remove nucleosomes from regions on which they intrinsically prefer not to reside and reposition them to energetically more favorable sites. This effect is opposite to that of Isw2, which moves nucleosomes to energetically disfavored positions within NDRs (Whitehouse and Tsukiyama, 2006). Asf1 serves as a histone chaperone during replication-dependent chromatin deposition and replication-independent histone exchange (De Koning *et al.*, 2007), raising the possibility that replication-independent histone exchange allows nucleosomes to find thermodynamically more favorable positions. This would account for the fact that predominantly unfavorably positioned nucleosomes are trapped in the *asf1* mutant, both during steady-state growth and following transcriptional reprogramming (Figure 3, B and D, and Figure S2B). Furthermore, we observed that nucleosome remodeling accompanying transcriptional reprogramming was delayed or diminished in extent in the *asf1* mutant (Figure 7C). This suggests that Asf1 participates in rapid nucleosome repositioning, which occurs too quickly to be associated with replication.

Swi/Snf possesses ATPase activity and thus could hypothetically move nucleosomes to energetically less favorable positions. However, since the excess nucleosome density during steady-state growth of the *snf2* mutant in glucose resides predominantly on less favorable sites (Figure 3A), the primary function of Swi/Snf appears to involve repositioning of kinetically trapped nucleosomes. Swi/Snf can unwrap nucleosomes in vitro (Lorch *et al.*, 1999; Clapier and Cairns, 2009), and this activity may serve in vivo to overcome the kinetic barrier to moving nucleosomes to their more favorable positions. Following transcriptional reprogramming during carbon source downshift, most of the energetically trapped nucleosomes are rapidly evicted, even in the absence of Snf2 activity. However, following this downshift, *snf2* mutants carry excess nucleosomes on energetically favorable sites (Figure 3C). This would suggest that under this condition Swi/Snf expends energy to move nucleosomes to less favorable sites, perhaps to effect regulatory reconfigurations of chromatin at specific promoters.

Asf1 and nucleosome exchange

Both Dion *et al.* (2007) and Rufiange *et al.* (2007) documented replication-independent nucleosome exchange across the genome and demonstrated that histone exchange occurs more extensively over promoters than in coding regions and that replacement rates over coding regions correlate with RNA polymerase II density. Moreover, Rufiange *et al.* (2007) provided evidence that loss of Asf1 activity significantly diminished histone replacement, a result consistent with the observation that Asf1 travels with RNA polymerase II and participates in eviction and reassembly of H3/H4 during transcriptional elongation (Schwabish and Struhl, 2006). We observed an unexpected correlation between promoters affected by the loss of Asf1 and those with slow histone H3 turnover (Figure 6). As discussed in the preceding section, we suggest that this observation is consistent with the role of Asf1 in removing nucleosomes from kinetically trapped sites. Namely, for those promoters in which histone exchange readily occurs, Asf1 activity would not be required to achieve thermodynamic equilibrium. Only in those promoters in which exchange is low would Asf1 be required to remove trapped nucleosomes, and thus its effects would be most evident at promoters with low intrinsic turnover. While Asf1 is only one of the factors that promote replication-independent nucleosome exchange (Rufiange *et al.*, 2007), our results suggest that promoters with low turnover are relatively more dependent on Asf1 activity than those with higher turnover rates.

Transcriptional reprogramming precedes nucleosome remodeling

The results presented here and those from previous studies indicate that nucleosome repositioning associated with transcriptional reprogramming is either delayed or reduced in extent in both *asf1* and *snf2* mutants. For instance, eviction of nucleosomes under inducing conditions is significantly delayed at the *PHO5* and *HO* promoters in *asf1* mutants (Adkins *et al.*, 2004; Gkikopoulos *et al.*, 2009; Takahata *et al.*, 2009) and at the *PHO5*, *HO*, and *HSP12* promoters in *snf2* mutants (Erkina *et al.*, 2008; Gkikopoulos *et al.*, 2009). In addition, rapid nucleosome clearance from promoters of heat shock–inducible genes is on average delayed following heat shock in *snf2* mutants relative to wild-type, although the kinetics of remodeling at repressed genes are the same in the two strains (Shivaswamy and Iyer, 2008). Consistent with these observations, we find that nucleosome remodeling is reduced in extent or delayed in both *asf1*Δ and *snf1*Δ strains relative to wild-type (Figure 7, C and D). Moreover, the exposure of transcriptional activator motifs at induced promoters is significantly less in *asf1* mutants and somewhat less in *snf2* mutants (Figure S7, B and E). At repressed promoters, the nucleosome occlusion of motifs associated with deactivated transcription factors is also less pronounced in mutant strains, although not as dramatically (Figure S7, C and F). Thus efficient nucleosome depletion during induction and nucleosome addition during repression both require histone chaperone and nucleosome remodeling activities.

Despite the smaller extent of nucleosome reorganization at promoters during induction and repression in *snf2* and *asf1* mutants, we observe very little change in the kinetics of transcriptional reprogramming in the mutants (Figure S6A). The kinetics of transcriptional changes in the *asf1* mutant following carbon upshift mirrors that of the wild-type under similar conditions, with a correlation coefficient of 0.95. Similarly, the pattern of expression in the *snf2* mutant following a glucose downshift strongly resembles that seen in wild-type cells with, if anything, accelerated repression of RP and Ribi genes and accelerated induction of stress-response genes in the *snf2* mutant relative to wild-type. These results broadly agree with those reported previously for global transcriptional changes following heat shock or entry into stationary phase of *snf2*, in which the pattern of changes in transcript levels was similar to that of wild-type cells (Shivaswamy and Iyer, 2008). Thus our results suggest that, while the extent of chromatin remodeling is significantly smaller in *asf1* or *snf2* mutants upon carbon source transitions, these mutants have little effect on the transcriptional reprogramming caused by the change in conditions.

Our results do not indicate that *asf1* and *snf2* mutants have no effect on transcription. As reported previously, we find that under steady-state conditions the expression of a number of genes is affected by deletion of *SNF2* or *ASF1*. For instance, *HO* expression is reduced ~20-fold in *snf2*Δ versus wild-type cells, consistent with the role of Snf2 in clearing nucleosomes from the *HO* URS2 during cell cycle activation of the gene (Gkikopoulos *et al.*, 2009; Takahata *et al.*, 2009). Rather, our results suggest that on average transcriptional reprogramming under carbon source transition proceeds normally in *snf2* and *asf1* mutants, despite delayed or diminished chromatin remodeling across the genome.

Our findings are consistent with the view that nucleosomal repositioning does not dictate transcriptional changes—rather, transcriptional reprogramming may occur before, and perhaps induce, nucleosome repositioning. Nucleosome remodeling factors such as Snf2 and histone chaperones such as Asf1 may be required to implement that repositioning. Previous results have suggested that remodeling complexes are recruited to promoters through physical interaction with transcription factors (Neely *et al.*, 1999; Yudkovsky *et al.*, 1999; Miller and Widom, 2003; Clapier and Cairns, 2009). Our results imply that this association is not required for transcriptional reprogramming caused by transcription factor binding. Rather, the association of the remodeling factors may institutionalize a new transcriptional program by reinforcing the new pattern through reconfiguration of the promoter chromatin structure to reflect the new regulatory state.

MATERIALS AND METHODS

Predicting nucleosome formation energies from a large-scale map of nucleosomes assembled in vitro on genomic DNA

A large-scale map of nucleosomes reconstituted in vitro on *S. cerevisiae* genomic DNA was obtained from Zhang *et al.* (2009). The map consists of 25 base pair–long sequence reads totaling 3,239,990 (0.27 reads per base pair) mapped to the *S. cerevisiae* genome (*Saccharomyces* Genome Database April 2008 build: http://www.yeastgenome.org). The map was used to build a biophysical model of nucleosome positioning and energetics as previously described (Locke *et al.*, 2010). Briefly, we assumed that genomic coordinates of mapped sequence reads define nucleosome positions on the yeast genome. We extended all mapped reads to the 147–base pair canonical nucleosome length and combined read counts from both strands, creating a sequence read profile (the number of nucleosomes that start at each genomic base pair) and a nucleosome coverage profile (the number of nucleosomes that cover a given base pair). We observed large gaps in the sequence read profile, possibly due to repetitive regions in the genome to which reads cannot be mapped, or to sequencing artifacts. We considered any stretch of ≥1000 base pairs without any mapped reads to be anomalous and excluded such regions from further analysis. We also found regions where the read coverage was uncharacteristically high. To mark such regions, we first found the average number of reads per base pair for each chromosome. Next, for each base pair, we calculated the running average number of reads in a window extending 75 base pairs in each direction. If this running average was more than three times the chromosomal mean, we flagged the region that extended out from the identified point in both directions until the running average equaled the mean, and removed this region from further consideration. We then created a filter that marked the union of all excluded regions. Finally, each excluded region was extended 146 base pairs upstream, so there was no contribution to the nucleosome energy from filtered regions.

The sequence read and nucleosome coverage profiles filtered in this way were smoothed by replacing the number of nucleosomes starting at each base pair with a $\sigma = 20$ Gaussian curve centered on that base pair. The area under the Gaussian curve was set equal to the number of sequence reads starting at that position. Next the sequence read and nucleosome coverage profiles were divided by the highest value of the nucleosome coverage on each chromosome, yielding the probability that a nucleosome would start at a given base pair (the nucleosome probability profile) and the probability that a given base pair is covered by any nucleosome (the nucleosome occupancy profile).

Free energies of nucleosome formation were derived from the nucleosome probability and occupancy profiles under the assumption that observed nucleosome positions were affected solely by intrinsic histone–DNA interactions and steric exclusion, in analogy with the fluid of finite-size one-dimensional particles in an arbitrary external potential (Percus, 1976):

$$\frac{E_i-\mu}{k_BT}=\log\frac{1-O_i+P_i}{P_i}+\sum_{j=i}^{i+146}\log\frac{1-O_j}{1-O_j+P_j} \quad (1)$$

where i = 1…L − 146 (L is the number of base pairs in the chromosome), E_i is the energy of a nucleosome starting at base pair i (i.e., occupying base pairs i …i + 146), μ is the chemical potential of histone octamers, k_BT is the product of the Boltzmann constant and room temperature, P_i is the probability to start a nucleosome at base pair i, and O_i is the nucleosome occupancy of base pair i, defined as

$$O_i=\sum_{j=i-146}^{i}P_j \quad (2)$$

We correlate nucleosome energies from Eq. (1) with DNA sequence features using a linear model fit:

$$\frac{E_i-\mu}{k_BT}=\varepsilon^0+\sum_{\alpha}n_\alpha^i\varepsilon_\alpha+\sum_{\alpha,\beta}n_{\alpha\beta}^i\varepsilon_{\alpha\beta}+r_i \quad (3)$$

where $\alpha,\beta=\{A,C,G,T\}$, ε^0 is the sequence-independent offset, n_α^i and $n_{\alpha\beta}^i$ are the number of mono- and dinucleotides found within the nucleosomal site occupying base pairs i …i + 146, and r_i is the residual. ε_α and $\varepsilon_{\alpha\beta}$ are the fitting parameters constrained to produce a hierarchical expansion in which dinucleotide parameters are only required to fit higher-order contributions not captured at the mononucleotide level: $\sum_\alpha\varepsilon_\alpha=0$, $\sum_\alpha\varepsilon_{\alpha\beta}=0$, $\sum_\beta\varepsilon_{\alpha\beta}=0$. As a result, the model has 13 free parameters (ε^0, three ε_α , and nine $\varepsilon_{\alpha\beta}$), 12 of which describe the energies of mono- and dinucleotide words. Note that in this model a given word is assigned the same energy regardless of its position within the nucleosomal site—we found that this simple approach predicts nucleosome occupancies nearly as well as more complex fits that take periodic dinucleotide distributions and longer words into account (Locke *et al.*, 2010). To account for frequency biases at the edges, we exclude all words that extend into 3 terminal base pairs on each end of the 147–base pair nucleosomal site from our counts.

Yeast strains

The *asf1*Δ strain was created by isolating genomic DNA from an *asf1*::KanMX strain (Winzeler *et al.*, 1999) and amplifying a PCR product across the *asf1*::KanMX locus, using primers asf1-F (5′-GCAGCCTTGCCTGACTTTAC-3′) and asf1-R (5′-ACCTCTCTTGCAGGTACCATT-3′). The PCR product was transformed into diploid strain Y3743 (*gal1*::*HIS3*/*gal1*::*TRP1 ade2–1/ade2–1 can1–100/can1–100 his3–11,15/his3–11,15 leu2–3112/leu2–3112 trp1–1/trp1–1 ura3–1/ura3–1*) and dissected to isolate Y3744 (*gal1*::*HIS3 ade2–1 can1–100 his3–11,15 leu2–3112 trp1–1 ura3–1 GAL asf1*::KANMX). Strains FY2 (*MAT*α *ura3–52*) and FY31 (*MAT*α *snf2*Δ*1*::*HIS3 ura3–52 his3*Δ*200*) (Sudarsanam *et al.*, 2000) were obtained from F. Winston (Department of Genetics, Harvard Medical School, Boston, MA).

Nucleosomal DNA isolation and hybridization

Mononucleosomal DNA from *asf1*Δ yeast and the wild-type reference strain was isolated as previously described (Zawadzki *et al.*, 2009). Briefly, 2 l of yeast was grown at 30°C in SC + 3% glycerol to a density of 2–3 × 10^6 cells/ml, at which point a zero-minute sample of 650 ml was removed. Glucose (2%) was added to the remaining culture and, after 20 min, 650 ml samples were removed. Yeast cells were formaldehyde cross-linked, converted to spheroplasts, then resuspended in NP buffer, and micrococcal nuclease (Sigma-Aldrich, St. Louis, MO) was added. DNA–protein cross-links were reversed by incubation at 65°C for at least 4 h. DNA was then purified by PCR clean-up kit (Qiagen, Valencia, CA), and the sample was analyzed by gel electrophoresis to ensure that the extent of digestion did not vary significantly from sample to sample (Figure S1). In addition, mononucleosomal DNA from the *asf1*Δ strain, the *snf2*Δ strain FY31, and the wild-type reference strain FY2 was isolated as above, except that yeast cells were grown in 1 l SC + 2% glucose media to a density of (2–3) × 10^6 cells/ml. Yeast cells from 500 ml of culture were collected by filtration, washed with SC + 2% glucose, resuspended in 500 ml SC + 2% glucose, then cross-linked immediately to provide the zero-minute time point. Yeast cells from the remaining 500 ml of culture were collected by filtration, washed with SC + 3% glycerol, then resuspended in 500 ml SC + 3% glycerol and grown for 20 min at 30°C before cross-linking. Mononucleosomal DNA was hybridized to Affymetrix (Santa Clara, CA) 1.0R yeast tiling arrays and processed with Affymetrix Tiling Array Software as previously described, producing log-intensity profiles (Zawadzki *et al.*, 2009). To ensure unbiased comparisons the mean log intensity for each chromosome has been subtracted from all profiles.

mRNA isolation and analysis

mRNA was isolated at several time points around the medium-to-medium transitions and hybridized to Agilent yeast oligo microarrays as described in Zaman *et al.* (2009). Quantitative real-time PCR reactions containing the SYBR Green Power Mix (Applied Biosystems, Bedford, MA) and gene-specific primers were performed using an Applied Biosystems 7900 instrument and reaction products analyzed by SDS software (Applied Biosystems). Relative mRNA levels were calculated by first determining the ratio of target RNA to ACT1 mRNA in each sample and then normalizing that value in samples from posttransition time points to that in the zero-minute (steady-state) sample.

Data used in this study are available at http://nucleosome.rutgers.edu.

ACKNOWLEDGMENTS

We gratefully acknowledge Donna Storton and Jessica Buckles for assistance with tiling microarrays, John Matese for management of the microarray data, and Soyeon Lippman for assistance with RNA profiling for *asf1* strains. This research was supported by NIH grants GM076562 and GM045840 to J.R.B. and HG004708 to A.V.M. and a Center for Quantitative Biology/NIH grant P50 GM071508. A.V.M. was also supported by an Alfred P. Sloan Research Fellowship. The funders had no role in study design, data collection and analysis, decision to publish, or preparation of the manuscript.

REFERENCES

Adkins MW, Howar SR, Tyler JK (2004). Chromatin disassembly mediated by the histone chaperone Asf1 is essential for transcriptional activation of the yeast PHO5 and PHO8 genes. Mol Cell 14, 657–666.

Adkins MW, Williams SK, Linger J, Tyler JK (2007). Chromatin disassembly from the PHO5 promoter is essential for the recruitment of the general transcription machinery and coactivators. Mol Cell Biol 27, 6372–6382.

Bryant GO, Prabhu V, Floer M, Wang X, Spagna D, Schreiber D, Ptashne M (2008). Activator control of nucleosome occupancy in activation and repression of transcription. PLoS Biol 6, 2928–2939.

Cairns BR (2009). The logic of chromatin architecture and remodelling at promoters. Nature 461, 193–198.

Chung HR, Vingron M (2009). Sequence-dependent nucleosome positioning. J Mol Biol 386, 1411–1422.

Clapier CR, Cairns BR (2009). The biology of chromatin remodeling complexes. Annu Rev Biochem 78, 273–304.
De Koning L, Corpet A, Haber JE, Almouzni G (2007). Histone chaperones: an escort network regulating histone traffic. Nat Struct Mol Biol 14, 997–1007.
Dion MF, Kaplan T, Kim M, Buratowski S, Friedman N, Rando OJ (2007). Dynamics of replication-independent histone turnover in budding yeast. Science 315, 1405–1408.
Driscoll R, Hudson A, Jackson SP (2007). Yeast Rtt109 promotes genome stability by acetylating histone H3 on lysine 56. Science 315, 649–652.
Erkina TY, Tschetter PA, Erkine AM (2008). Different requirements of the SWI/SNF complex for robust nucleosome displacement at promoters of heat shock factor and Msn2- and Msn4-regulated heat shock genes. Mol Cell Biol 28, 1207–1217.
Field Y, Kaplan N, Fondufe-Mittendorf Y, Moore IK, Sharon E, Lubling Y, Widom J, Segal E (2008). Distinct modes of regulation by chromatin encoded through nucleosome positioning signals. PLoS Comput Biol 4, e1000216.
Fillingham J *et al*. (2009). Two-color cell array screen reveals interdependent roles for histone chaperones and a chromatin boundary regulator in histone gene repression. Mol Cell 35, 340–351.
Gkikopoulos T, Havas KM, Dewar H, Owen-Hughes T (2009). SWI/SNF and Asf1p cooperate to displace histones during induction of the *Saccharomyces cerevisiae* HO promoter. Mol Cell Biol 29, 4057–4066.
Han J, Zhou H, Horazdovsky B, Zhang K, Xu RM, Zhang Z (2007). Rtt109 acetylates histone H3 lysine 56 and functions in DNA replication. Science 315, 653–655.
Hartley PD, Madhani HD (2009). Mechanisms that specify promoter nucleosome location and identity. Cell 137, 445–458.
Huisinga KL, Pugh BF (2004). A genome-wide housekeeping role for TFIID and a highly regulated stress-related role for SAGA in *Saccharomyces cerevisiae*. Mol Cell 13, 573–585.
Kaplan N *et al*. (2009). The DNA-encoded nucleosome organization of a eukaryotic genome. Nature 458, 362–366.
Korber P, Barbaric S, Luckenbach T, Schmid A, Schermer UJ, Blaschke D, Horz W (2006). The histone chaperone Asf1 increases the rate of histone eviction at the yeast PHO5 and PHO8 promoters. J Biol Chem 281, 5539–5545.
Korber P, Luckenbach T, Blaschke D, Horz W (2004). Evidence for histone eviction in *trans* upon induction of the yeast *PHO5* promoter. Mol Cell Biol 24, 10965–10974.
Lam FH, Steger DJ, O'Shea EK (2008). Chromatin decouples promoter threshold from dynamic range. Nature 453, 246–250.
Liu X, Lee CK, Granek JA, Clarke ND, Lieb JD (2006). Whole-genome comparison of Leu3 binding in vitro and in vivo reveals the importance of nucleosome occupancy in target site selection. Genome Res 16, 1517–1528.
Locke G, Tolkunov D, Moqtaderi Z, Struhl K, Morozov AV (2010). High-throughput sequencing reveals a simple model of nucleosome energetics. Proc Natl Acad Sci USA 107, 20998–21003.
Lorch Y, Zhang M, Kornberg RD (1999). Histone octamer transfer by a chromatin-remodeling complex. Cell 96, 389–392.
Martens JA, Winston F (2003). Recent advances in understanding chromatin remodeling by Swi/Snf complexes. Curr Opin Genet Dev 13, 136–142.
Mavrich TN, Ioshikhes IP, Venters BJ, Jiang C, Tomsho LP, Qi J, Schuster SC, Albert I, Pugh BF (2008). A barrier nucleosome model for statistical positioning of nucleosomes throughout the yeast genome. Genome Res 18, 1073–1083.
Mellor J, Morillon A (2004). ISWI complexes in *Saccharomyces cerevisiae*. Biochim Biophys Acta 1677, 100–112.
Miller JA, Widom J (2003). Collaborative competition mechanism for gene activation in vivo. Mol Cell Biol 23, 1623–1632.
Morse RH (2007). Transcription factor access to promoter elements. J Cell Biochem 102, 560–570.
Nagalakshmi U, Wang Z, Waern K, Shou C, Raha D, Gerstein M, Snyder M (2008). The transcriptional landscape of the yeast genome defined by RNA sequencing. Science 320, 1344–1349.
Neely KE, Hassan AH, Wallberg AE, Steger DJ, Cairns BR, Wright AP, Workman JL (1999). Activation domain-mediated targeting of the SWI/SNF complex to promoters stimulates transcription from nucleosome arrays. Mol Cell 4, 649–655.
Percus JK (1976). Equilibrium state of a classical fluid of hard rods in an external field. J Stat Phys 15, 505–511.
Rando OJ, Chang HY (2009). Genome-wide views of chromatin structure. Annu Rev Biochem 78, 245–271.
Rufiange A, Jacques PE, Bhat W, Robert F, Nourani A (2007). Genome-wide replication-independent histone H3 exchange occurs predominantly at promoters and implicates H3 K56 acetylation and Asf1. Mol Cell 27, 393–405.
Saha A, Wittmeyer J, Cairns BR (2006). Chromatin remodelling: the industrial revolution of DNA around histones. Nat Rev Mol Cell Biol 7, 437–447.
Schwabish MA, Struhl K (2006). Asf1 mediates histone eviction and deposition during elongation by RNA polymerase II. Mol Cell 22, 415–422.
Segal E, Fondufe-Mittendorf Y, Chen L, Thastrom A, Field Y, Moore IK, Wang JP, Widom J (2006). A genomic code for nucleosome positioning. Nature 442, 772–778.
Shivaswamy S, Bhinge A, Zhao Y, Jones S, Hirst M, Iyer VR (2008). Dynamic remodeling of individual nucleosomes across a eukaryotic genome in response to transcriptional perturbation. PLoS Biol 6, e65.
Shivaswamy S, Iyer VR (2008). Stress-dependent dynamics of global chromatin remodeling in yeast: dual role for SWI/SNF in the heat shock stress response. Mol Cell Biol 28, 2221–2234.
Sudarsanam P, Iyer VR, Brown PO, Winston F (2000). Whole-genome expression analysis of snf/swi mutants of *Saccharomyces cerevisiae*. Proc Natl Acad Sci USA 97, 3364–3369.
Sudarsanam P, Winston F (2000). The Swi/Snf family nucleosome-remodeling complexes and transcriptional control. Trends Genet 16, 345–351.
Takahata S, Yu Y, Stillman DJ (2009). FACT and Asf1 regulate nucleosome dynamics and coactivator binding at the HO promoter. Mol Cell 34, 405–415.
Tillo D, Hughes TR (2009). G+C content dominates intrinsic nucleosome occupancy. BMC Bioinformatics 10, 442.
Tolkunov D, Morozov AV (2010). Genomic studies and computational predictions of nucleosome positions and formation energies. Adv Protein Chem Struct Biol 79, 1–57.
Travers A, Caserta M, Churcher M, Hiriart E, Di Mauro E (2009). Nucleosome positioning—what do we really know? Mol Biosyst 5, 1582–1592.
Whitehouse I, Rando OJ, Delrow J, Tsukiyama T (2007). Chromatin remodelling at promoters suppresses antisense transcription. Nature 450, 1031–1035.
Whitehouse I, Tsukiyama T (2006). Antagonistic forces that position nucleosomes in vivo. Nat Struct Mol Biol 13, 633–640.
Williams SK, Truong D, Tyler JK (2008). Acetylation in the globular core of histone H3 on lysine-56 promotes chromatin disassembly during transcriptional activation. Proc Natl Acad Sci USA 105, 9000–9005.
Winzeler EA *et al*. (1999). Functional characterization of the *S. cerevisiae* genome by gene deletion and parallel analysis. Science 285, 901–906.
Yudkovsky N, Logie C, Hahn S, Peterson CL (1999). Recruitment of the SWI/SNF chromatin remodeling complex by transcriptional activators. Genes Dev 13, 2369–2374.
Zaman S, Lippman SI, Schneper L, Slonim N, Broach JR (2009). Glucose regulates transcription in yeast through a network of signaling pathways. Mol Syst Biol 5, 245.
Zawadzki KA, Morozov AV, Broach JR (2009). Chromatin-dependent transcription factor accessibility rather than nucleosome remodeling predominates during global transcriptional restructuring in *Saccharomyces cerevisiae*. Mol Biol Cell 20, 3503–3513.
Zhang Y, Moqtaderi Z, Rattner BP, Euskirchen G, Snyder M, Kadonaga JT, Liu XS, Struhl K (2009). Intrinsic histone-DNA interactions are not the major determinant of nucleosome positions in vivo. Nat Struct Mol Biol 16, 847–852.